J Solid State Electrochem (2004) 8: 727–734
DOI 10.1007/s10008-004-0538-5

ORIGINAL PAPER

X. D. Dang · C. M. Intelmann · U. Rammelt · W. Plieth

Electrochemical copolymerization of pyrrole and 2,2-bithiophene and semiconducting characterization of the resulting copolymer films by electrochemical impedance spectroscopy and photoelectrochemistry

Received: 10 March 2004 / Accepted: 8 April 2004 / Published online: 3 August 2004

Abstract The electrochemical copolymerization of pyrrole and bithiophene was studied at a polymerization potential of 1.1 V for various monomer ratios. The cyclic voltammograms showed that the electrochemical properties of the resulting copolymer films changed gradually from those of polypyrrole to polybithiophene with an increase in concentration of bithiophene in the initial electrolyte. The evidence for copolymer formation is based on the analytical results of electrospray ionization mass spectroscopy, thermoanalysis, and Raman spectroscopy. The results showed that cooligomers and homooligomers were found in the electrolyte after copolymerization. The difference between the morphology of a copolymer of pyrrole and bithiophene and a polymer mixture of polypyrrole and polythiophene was demonstrated by scanning electron microscopy. Electrochemical impedance and photocurrent measurements were carried out in order to achieve information on the semiconducting properties of the homopolymers and copolymers obtained. A model of a very thin layer of polypyrrole formed immediately on the electrode surface covered by a thicker copolymer film was developed to explain the results.

Keywords Copolymer · Organic semiconductor · Mass spectroscopy · Photocurrent · Electrochemical impedance spectroscopy

Dedicated to Zbigniew Galus on the occasion of his 70th birthday.

X. D. Dang · C. M. Intelmann · U. Rammelt · W. Plieth (✉)
Institute of Physical Chemistry and Electrochemistry,
Dresden University of Technology,
01062 Dresden, Germany
E-mail: waldfried.plieth@chemie.tu-dresden.de

Introduction

Conducting polymer-modified electrodes have been the subject of a great deal of recent investigations [1]. The structure and property of the polymer can be changed from a doped state as a conductor to an undoped (neutral) state as a copolymerization insulator or a semiconductor, and this is essentially dependent on the width of the band gap. Among these polymers, polythiophene derivatives [2, 3] have been investigated intensively, due to their electrical and optical properties as well as their stability. Polypyrrole [4, 5] is of particular interest since the films can be formed from aqueous and non-aqueous solutions at relatively low oxidation potentials of monomers.

One important aspect of conducting polymer technology is the modification and control of their electrical, optical and mechanical properties for specific technological applications. Electrochemical copolymerization – incorporation of two different monomers into the same polymer chain – is one strategy for developing new materials by combining individual properties of polymers [6]. Recent investigations into electrochemical copolymerization have centered on the influence of the electrolyte, the monomer ratio in the initial electrolyte, and the polymerization potential on the structure and properties of the copolymers [7, 8]. In the investigation presented here, spectroscopic techniques such as mass spectroscopy and thermoanalysis were applied to prove the copolymer formation. The semiconducting properties of homopolymers have been intensively investigated in aqueous and non-aqueous solutions [9, 10, 11, 12]; in this paper, the semiconducting behavior of the electrochemically prepared copolymer is studied.

The paper focuses on the fabrication and characterization of conducting copolymers based on pyrrole and bithiophene. Evidence of the copolymer formation is obtained via electrospray ionization mass spectroscopy, thermoanalysis, Raman spectroscopy, electrochemical impedance spectroscopy, and photoelectrochemistry.

Experimental

The electrolyte was 0.1 M tetrabutylammonium hexafluorophosphate $N(Bu)_4PF_6$ (Aldrich, 98%) in acetonitrile (Fischer, 99.9%) except for the electrospray ionization mass spectroscopy (ESI MS) where 0.1 M lithium perchlorate $LiClO_4$ (Fluka, 98%) was used. Pyrrole (Aldrich) was distilled in vacuum before each polymerization, and 2,2-bithiophene (Lancaster) was used as received. Copolymerization of pyrrole (Py) and bithiophene (BT) was performed under potential control using a three-electrode cell, Ar atmosphere and stirring. Platinum was used as the working (1 cm^2) and counter electrode (3.14 cm^2). Both electrodes were mounted at a fixed distance apart. A saturated calomel electrode (SCE, $E = 0.241$ V versus a normal hydrogen electrode) was the reference electrode (all potentials mentioned in this paper were related to the SCE). To prevent water diffusion from the reference electrode into the working electrolyte, an electrolyte bridge was used. The electrochemical behavior of homopolymer/copolymer films was characterized in monomer-free electrolyte after washing with acetonitrile to remove the remaining monomers and oligomers. The copolymer films were cycled to reach a stable condition in the potential range from -1.0 V to $+1.25$ V, which covers the redox potentials of both PPy and PBT, at a scan rate of 50 mV/s. All electrochemical experiments were carried out with the same electrochemical cell using a potentiostat/galvanostat EG&G model 263A.

One strategy was used to determine the copolymer formation indirectly, which was synthesized electrochemically. The electrolyte after copolymerization was investigated by electrospray ionization mass spectroscopy (ESI MS, Hewlett-Packard-Bruker ESQUIRE LC-MS), using ammonium acetate as solvent. In order to avoid very strong signals coming from the supporting electrolyte 0.1 M $N(Bu)_4PF_6$, 0.1 M $LiClO_4$ was used for the ESI MS measurements.

Differential scanning calorimetry (DSC) measurements were performed with a METTLER DSC 30 operating at a heating rate of 5 K min^{-1} under N_2 atmosphere, with an empty aluminum pan used as reference.

Raman spectra of the obtained polymer films were recorded with a Renishaw Raman imaging microscope system 2000 using a He-Ne laser with wavelength of 633 nm, and using 1% laser power for PBT, 10% for PyBT20, and 50% for both PyBT10 and PPy films.

Elemental analysis of the copolymer samples was made on an elemental analyzer Euro EA 3000. In order to remove the supporting electrolyte $N(Bu)_4PF_6$ from the polymers before analyzing, they were reduced at a negative potential of -0.75 V. To extract remaining solvent and electrolyte, the samples were washed with methanol in Soxhlet for two days.

The morphologies of the homopolymer/copolymer films were characterized by scanning electron microscopy (ZEISS DSM 982 Gemini).

Electrochemical impedance spectroscopy (EIS) measurements were performed in monomer-free electrolyte with a three-electrode cell (area of working electrode 0.125 cm^2) with a Zahner-Electric IM6d impedance measurement system. An AC amplitude of 10 mV was applied and the data was taken in the frequency range of 0.1 Hz to 100 kHz. The impedance spectra of copolymer films were registered in the potential range that covers the redox potentials of both homopolymers (PPy and PBT). All polymer films were polarized at the oxidation potential for one hour, and then the potential was made more negative in steps of 50 mV. An equilibration time of 15 min at each applied potential was set before the measurement.

The photoelectrochemical spectra were registered in a three-electrode cell with an optical window. A 1000 W Xenon lamp was employed as a light source in combination with a Zeiss M4QIII grating monochromator and a PAR 197 light chopper with a frequency of 400 Hz. To polarize the polymer-modified electrode, a potentiostat HEKA model D 6734 potentostat/galvanostat was used. The photocurrent signal was registered via a PAR model 5208 lock-in amplifier. In order to improve photocurrent signals, the homopolymer/copolymer films were reduced in a monomer-free electrolyte solution and then washed with methanol before characterization. To compare the photoelectrochemical behavior, the photocurrent spectra were registered under the same conditions.

Results and discussion

Characterization of the resulting polymer films

Cyclic voltammograms

In order to determine the optimal conditions for copolymerization, the oxidation potentials of pyrrole (Py) and bithiophene (BT) were examined. The onset potentials of Py and BT for polymerization on platinum electrodes were 0.7 V and 1.0 V, respectively. Because of the small difference in oxidation potential of the monomers, copolymerization should be possible. Copolymers were synthesized at the fixed potential of 1.1 V from acetonitrile solution containing 0.01 M Py and 0.1 M BT (ratio [Py]/[BT] = 1/10, short name PyBT10), and 0.01 M Py and 0.2 M BT (ratio [Py]/[BT] = 1/20, short name PyBT20), respectively.

Cyclic voltammograms (CVs) of the resulting polymer films in monomer-free electrolyte are given in Fig. 1. Curves 1 and 4 are typical of the pure polypyrrole (PPy) and polybithiophene (PBT) in 0.1 M $N(Bu)_4PF_6$/acetonitrile solution. CVs for the copolymer films PyBT10 and PyBT20 are shown in curves 2 and 3, respectively. The redox potentials of polymer films PyBT10 and PyBT20 shifts from those of PPy to PBT with increasing concentration of BT in the initial electrolyte. On the other hand, the potential at which the

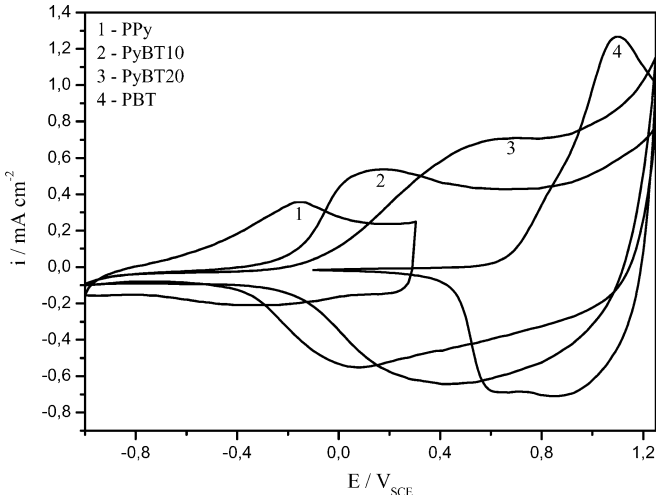

Fig. 1 CVs of polymer films synthesized at an E_{poly} of 1.1 V in monomer-free 0.1 M $N(Bu)_4PF_6$ solution, scan rate 50 mV/s

copolymer films are oxidized shifts from −0.33 V for PyBT10 to −0.13 V for PyBT20, whereas those potentials for PPy and PBT films are at −0.70 V and +0.60 V, respectively. As the concentration of BT increases, corresponding CVs of the resulting copolymer films change systematically from that of PPy to PBT due to the increase of BT groups in the copolymer film. If a polymer mixture of PPy and PBT is formed, it is expected that two oxidation peaks corresponding to two homopolymers should appear. This result is strong evidence that the copolymerization of Py and BT led to a true copolymer rather than a polymer mixture.

ESI mass spectroscopy

P. A. Aubert et al [13] showed that two oxidation peaks corresponding to homopolymers were still found when a copolymer film was produced from the monomers pyrrole and nickel-6,6′-bis(2-hydroxyphenyl)bipyridine. This could be explained by two blocks in the copolymer chain, which are of nearly the same electroactivity but differ much in redox potential. From this point of view, if a true copolymer was synthesized, cooligomers with various monomer units of Py and BT after copolymerization should be found in the electrolyte. In order to prove this assumption, ESI spectra of the electrolyte after copolymerization were measured. The ESI spectra clearly indicated that cooligomers of various compositions Py_xBT_y were formed in the electrolyte containing 0.01 M Py and 0.1 M BT after copolymerization at an E_{poly} of 1.1 V. Values of some typical peaks and their assignments are summarized in Table 1. Though the concentration of BT is ten times higher than that of Py in the starting electrolyte, cooligomers containing several Py units were observed. In fact, this is not surprising because the reactivity of BT is significantly lower than that of Py under these reaction conditions [14]. Oligomers Py_{11} (m/z 720.3) and BT_3 (m/z 517) were also found. Therefore, copolymers containing more Py units as well as corresponding homopolymers were formed at a potential of 1.1 V.

Table 1 Values of some typical peaks and their assignments in the ESI mass spectrum of acetonitrile solution containing 0.1 M $LiClO_4$ and 0.01 M Py and 0.1 M BT after copolymerization at E_{poly} of 1.1 V, positive mode

Value of m/z	Assignment	Exact m/z
248.8	$Py_1BT_1NH_4^+$	249.1
335.9	$Py_2BT_1H^+K^+$	336.0
428.0	$Py_4\ BT_12H^+$	428.1
517.2	BT_3Na^+	517.0
568.2	$Py_1BT_3H^+Li^+$	568.0
644.1	$Py_7BT_1Na^+$	644.2
720.3	$Py_{11}3H^+$	720.3
811.8	$Py_2BT_4H^+Na^+$	812.0
895.5	$Py_{11}BT_12Li^+$	895.3
998.6	$Py_{10}BT_2NH_4^+$	998.3
1148.6	$Py_5BT_52H^+$	1159.0

Thermoanalysis

Differential scanning calorimetry (DSC) measurements were used as another test of copolymer formation. It is expected that two glass transition temperatures (T_g) should be found for a polymer mixture between PPy and PBT. The values of T_g for PPy, PyBT10 and PBT were found to be 81, 88 and 92 °C, respectively. The shift of T_g for the copolymer PyBT10 can be explained by the chemical structure that affects the mobility of the polymer chain [15].

Raman spectroscopy

Fig. 2 represents the Raman spectra of the homopolymer/copolymer films. The spectral data is interpreted by

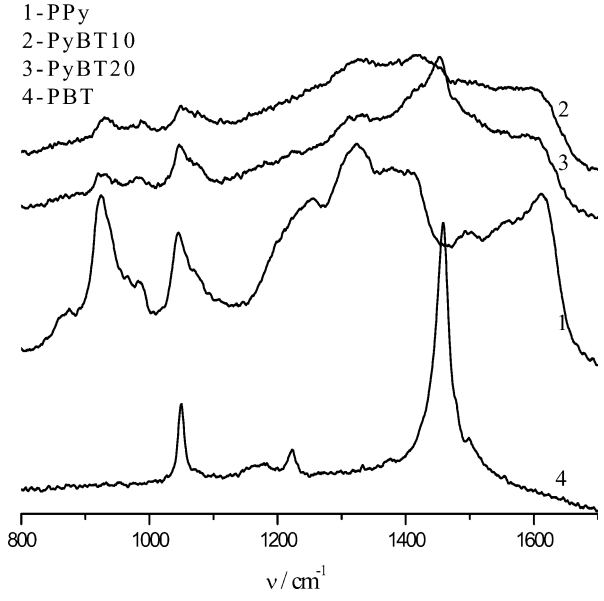

Fig. 2 Raman spectra of polymer films synthesized at an E_{poly} of 1.1 V

Table 2 The composition of copolymers synthesized from the electrolyte containing 0.01 M Py and 0.1 M BT (sample PyBT10), and 0.01 M Py and 0.2 M BT (sample PyBT20) at the E_{poly} of 1.1 V

Sample	Polymer % weight			mol%Py
	%C	%N	%S	
PyBT10	56.0	9.0	10.7	71
PyBT20	56.4	7.7	15.7	63

analogy with the reported Raman data on PPy [16, 17] and PBT [18, 19]. Changes of Raman spectra in the frequency range from 1300–1500 cm^{-1} related to C–C stretching, C–N stretching, and C=C symmetric stretching, and in the frequency range from 900–1100 cm^{-1} related to ring antisymmetric deformation and C–H bending are observed. The spectra of the copolymer resemble the spectra of the PPy more than those of the PBT. Characteristic differences are missing bands in the copolymer spectra compared with the PPy (860, 1250 and 1380 cm^{-1}) and with the PBT (1170 and 1220 cm^{-1}). A new feature of the copolymer spectra is the shoulder at 1337 cm^{-1}. The intensity of the band at 1458 cm^{-1} (assigned to C=C symmetric stretching of the thiophene ring) increases with an increase in concentration of BT in the initial electrolyte. On the other hand, the intensity ratio between the vibration at 1050 cm^{-1}, related to C–H plane symmetric deformation, and the vibration at 925 cm^{-1} assigned to ring antisymmetric deformation of Py, increases as the concentration of Py is reduced. It is possible to confirm the expected trend described at the beginning of the "Results" section later: the higher the concentration of BT in the initial electrolyte, the greater the similarity of the Raman spectra of the copolymer and PBT films.

Elemental analysis

The data from the elemental analysis of the copolymers are shown in Table 2. In order to determine the copolymer composition, the mole percent of pyrrole was calculated using the following equation [20]:

$$\text{mole \% Py} = \frac{96.089\ (\text{N}/\text{C})}{14.007 + 48.044\ (\text{N}/\text{C})} \quad (1)$$

where the ratio (N/C) was obtained by inserting the respective weight percent values taken from of Table 2.

At a copolymerization potential of 1.1 V, the Py content in the resulting copolymers decreased from 71% for PyBT10 to 63% for PyBT20. If two monomers were of similar reactivity, then the composition of the copolymer would be the same as that of the solution from which the copolymer was formed. However, BT is much less reactive than Py under the same experimental conditions [14]. Therefore, Py is still in excess in the copolymer.

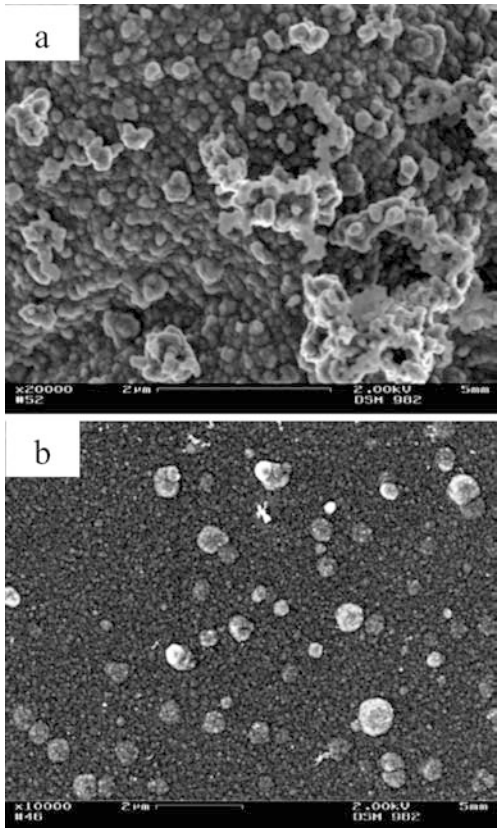

Fig. 3 SEM micrographs. Polymer films were deposited in acetonitrile solution containing 0.1 M $N(Bu)_4PF_6$. **a** Copolymer PyBT20 synthesized at E_{poly} of 1.1 V from the electrolyte containing 0.01 M pyrrole and 0.2 M bithiophene. **b** Polymeric mixture (polypyrrole and polythiophene) synthesized by cyclic voltammetry in the potential range of −0.75 to +1.6 V from the electrolyte containing 1.5×10^{-3} M pyrrole and 0.1 M thiophene, scan rate 50 mV/s

SEM micrographs

In Fig. 3a, a homogeneous and compact film of the copolymer PyBT20 synthesized from the electrolyte containing 0.01 M pyrrole and 0.2 M bithiophene is shown. This morphology is different from that of a polymer mixture of polypyrrole and polythiophene synthesized from the electrolyte containing 1.5×10^{-3} M and 0.1 M thiophene (Fig. 3b). In this case, it does not seem possible to prepare a copolymer because of the large difference in the oxidation potentials between the monomers. Consequently, polythiophene clusters were deposited on the polypyrrole film. In order to support this by an analytical method, EDX was employed. The result showed that sulfur was found in the polymer clusters, but not in the background polymer film.

Semiconducting properties

Electrochemical impedance spectroscopy

Figure 4 shows typical impedance spectra for PyBT20 in 0.1 M $N(Bu)_4PF_6$/acetonitrile at various potentials

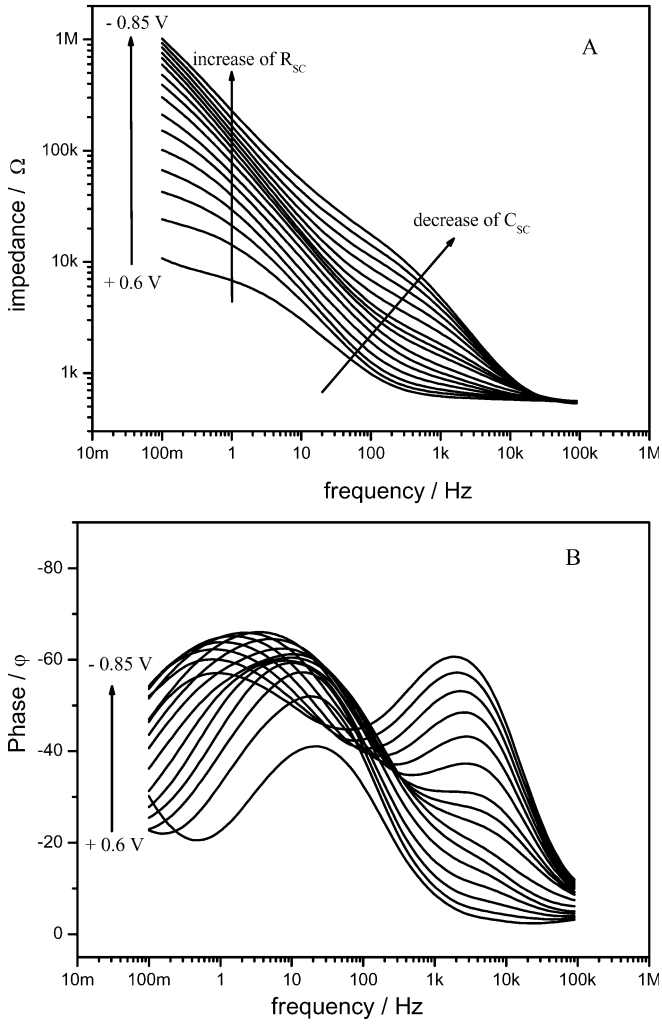

Fig. 4 Bode plots of PyBT20 film at different applied potentials (potential steps of 50 mV). A: Modulus of impedance; B: phase shift

during the reduction process of the copolymer film. The impedance spectra were registered in the potential range from +0.6 V to −0.85 V in potential steps of 50 mV. The impedance data can be analyzed with the equivalent circuit shown in Fig. 5. The model is that of a conducting polymer film in its semiconducting state. In the case of a copolymer film, two space charge capacitances

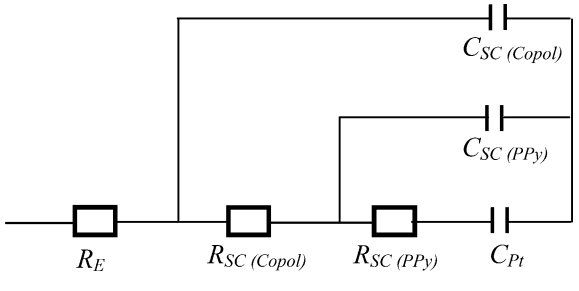

Fig. 5 Equivalent circuit for polymer PyBT20 (see text)

are observed. A possible explanation would be the deposition of a bilayer of PPy(homopolymer)/copolymer on the platinum electrode. The high frequency response of the system consists of the space charge capacitance $C_{SC\ (Copol)}$ of the copolymer in parallel with the corresponding space charge resistance $R_{SC\ (Copol)}$, whereas the low frequency response is due to the $C_{SC\ (PPy)}$ and $R_{SC\ (PPy)}$ of the homopolymer. R_E and C_{Pt} are the electrolyte resistance and the capacitance of the platinum electrode, respectively.

In order to fit the data, each capacitance in the equivalent circuit had to be replaced by a constant phase element CPE:

$$Z_{CPE} = A_{CPE}(j\omega)^{-n} \tag{2}$$

This replacement was necessary to take into account the non-ideal behavior of the polymer films, which is due to inhomogenities in the conductance or dielectric constant inside the layer, and the exponent n of the CPE element can be regarded as a measure of the inhomogenity of the copolymer film ($0.90 \le n \le 0.97$) [21]. The corrected values of the capacitances were obtained from the fitting program of Zahner elektrik, which uses the Z_{CPE} values for its calculation [22]. By plotting $1/C^2$ versus the applied potential E, a linear relationship is observed in the potential range from −0.2 V to −0.85 V for the high frequency capacitance and from −0.6 V to −0.85 V for the low frequency capacitance. In this potential range both capacitances are space charge capacitances C_{SC}, which obey the Mott-Schottky equation:

$$C_{SC}^{-2} = \left(\frac{2}{e\varepsilon\varepsilon_0 N}\right)\left(\frac{E - E_{FB} - kT}{e}\right) \tag{3}$$

where ϵ is the dielectric constant of the polymer film, ϵ_o the permittivity of free space, e the charge of the electron, N the doping concentration, E the applied potential and E_{FB} the flatband potential. At room temperature (25 °C), kT/e is 26 mV and can be neglected.

With both polymers, PyBT10 and PyBT20, the intercept of the straight line with the E axis gives two values of E_{FB}, as can be seen in Fig. 6. One value of E_{FB} shifts from that of pure PPy ($E_{FB} = -0.64$ V) to pure PBT ($E_{FB} = +0.34$ V) with an increase in concentration of BT in the initial electrolyte. It is suggested that this E_{FB} originates from the semiconducting characteristics of the copolymer film. The change of space charge capacitance was observed in a different potential range with changing copolymer composition. This observation is consistent with the shift of the redox potentials recorded by cyclic voltammetry. The other value of E_{FB} is always constant at a potential of −0.64 V and corresponds to the E_{FB} of pure PPy. This suggests that a thin PPy layer is produced in the first seconds of the copolymerization process and before the growth of copolymer because of the low oxidation potential of Py. In addition, the reactivity of radical cations of Py is significantly higher than that of BT under the same

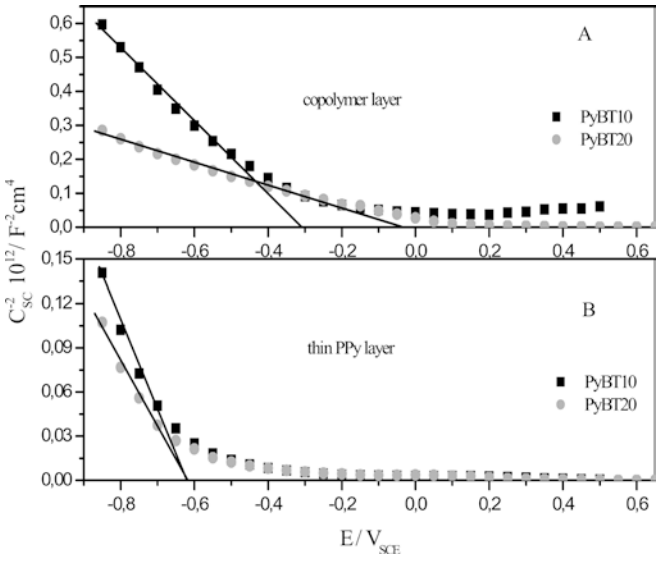

Fig. 6 Mott-Schottky plots of PyBT10 and PyBT20 films for capacitances evaluated at various frequency domains. A: high frequency region; B: low frequency region

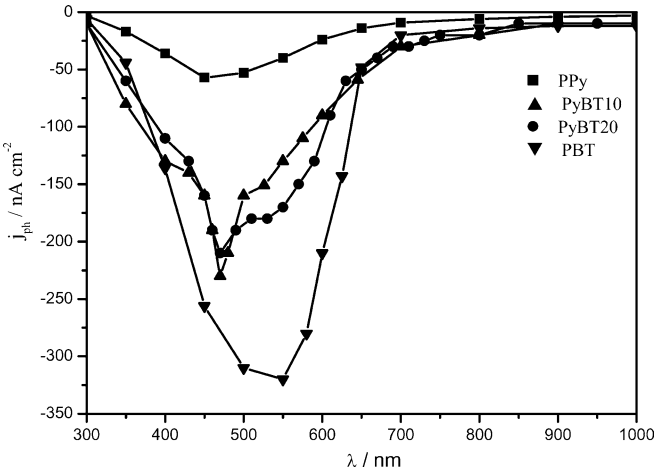

Fig. 7 The wavelength dependence of the cathodic photocurrent, at an applied potential of $E = -0.75$ V

conditions [14]. Therefore, first a very thin PPy layer is formed on the electrode surface instead of a true copolymer layer of Py and BT. The growth of the copolymer film takes place on the very thin PPy modified electrode. From this model it follows that the copolymer film is produced electrochemically from two monomers with different oxidation potentials as a bilayer.

The doping concentration N of polymer films was evaluated from the slope of the Mott-Schottky plot, neglecting some factors such as roughness and porosity of the polymer films and changes in the dielectric constant of the material as a function of its oxidation state. As summarized in Table 3 the N values are of the order of 10^{17} carriers/cm^3.

Photoelectrochemistry

The results for the impedance measurements were completed by the photocurrent measurements. The dependence of the photocurrent on the light energy at an applied potential is given in Fig. 7. The cathodic photocurrent of the photoelectrochemical spectra for the reduced polymer films is typical of a p-type semiconductor. The broad and pronounced maxima can be interpreted by π–π^* transitions. For PyBT10 and PyBT20 a maximum was observed at a wavelength of 470 nm with shoulders at 512 nm and 525 nm, respectively. This shoulder shifts toward the maximum of PBT (550 nm) as the BT content in the copolymer film increases.

By employing the Gärtner model [23] for charge separation across an interface, and assuming that $1/\alpha \gg L_p$ (diffusion length of minority carriers) and $1/\alpha \gg W_{SC}$ (thickness of the space charge layer). The relationship between the photocurrent j_{ph} and photon energy hv is

$$(j_{ph}\, hv)^{2/m} = A(hv - E_g) \tag{4}$$

where α is absorption coefficient, E_g is the band gap energy and A is a constant. $m = 1$ and $m = 4$ describe direct and indirect transitions, respectively.

The plots of $(j_{ph}hv)^2$ versus hv show linear regions from 500–700 nm (Fig. 8) and confirm a direct band gap E_g^{di} at the interception point with the hv axis. When the mole%Py drops from 71% in copolymer PyBT10 to 63% in copolymer PyBT20, the E_g^{di} drops from 1.97 eV to 1.94 eV, respectively. For comparison, the E_g^{di} for pure PPy and PBT is also shown in Table 3.

Figure 9 shows the dependence of the photocurrent of the polymer films on the applied potential. The onset photocurrent of the very thin PPy layer on the electrode surface could not be found due to the influence of the photocurrent generated by the copolymer film. At applied potentials more positive than E_{FB} of pure PPy (−0.64 V), a thin PPy layer can be regarded as a conductive electrode. Therefore, the photocurrent signals for polymer films PyBT10 and PyBT20 were generated

Table 3 Semiconducting parameters of polymer films synthesized at E_{poly} of 1.1 V

PEC: photoelectrochemistry; EIS: electrochemical impedance spectroscopy; [a] values of the thin PPy layer; [b] values of the copolymer layer

Sample	E_g^{di}(eV)	Flat band potential E_{FB}/V		Doping concentration N (carriers/cm^3)
		PEC	EIS	
PPy	2.07	−0.55	−0.64	$1.0\ 10^{17}$
PyBT10	1.97	−0.30	−0.64[a]; −0.34[b]	2.5×10^{17}, [a]; 1.4×10^{17}, [b]
PyBT20	1.94	−0.08	−0.64[a]; −0.05[b]	3.2×10^{17}, [a]; 4.6×10^{17}, [b]
PBT	1.92	+0.48	+0.35	3.5×10^{17}

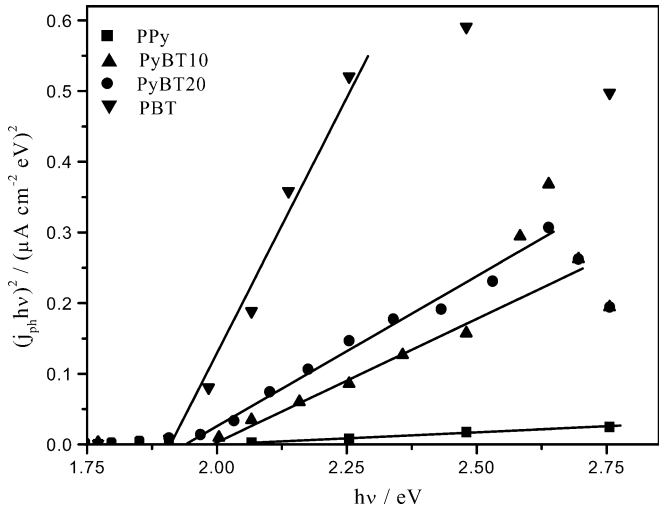

Fig. 8 $(j_{ph}hv)^2$ versus hv for determining E_g^{di} of the polymer films

by the separation of electron-hole pairs in the space charge region of the copolymer film. The onset potential of photocurrent spectra shifts from that of copolymer PyBT10 (−0.30 V) to PyBT20 (−0.08 V) when the BT content in the copolymer film increases from 29% to 37%, respectively. Those values are nearly 100 mV more positive than the E_{FB} values obtained from impedance measurements [22].

Band energy diagram

The p-type polymer semiconductor/electrode and p-type polymer semiconductor/electrolyte junctions are described in the literature [24]. The flat band potential is approximately equal to the Fermi level E_F [25]. The difference between the Fermi level and the top of the valence band is approximately 0.2 eV [26]. Converting potential values into energy values, the equation is used is [27]:

$$E\ (\text{eV}) = -4.5 - E(\text{V vs NHE})$$

As discussed, the copolymer of Py and BT produced electrochemically on a platinum electrode can be regarded as a bilayer. The results of the experiments are summarized in Fig. 10. The thin PPy layer can be regarded as a conductive electrode if the applied potential is more positive than the E_{FB} of PPy (−0.64 V). In this case, the contact characteristic of platinum and the thin PPy layer is ohmic. The cathodic photocurrent is generated by the separation of electron-hole pairs in the space charge region of the copolymer.

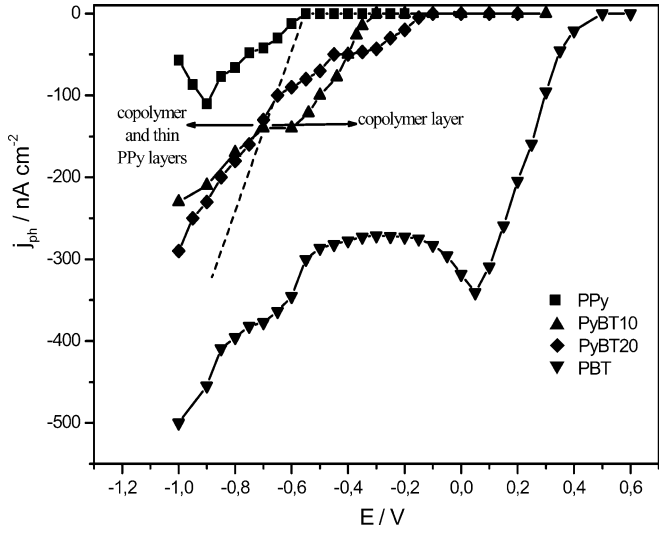

Fig. 9 The potential dependence of the cathodic photocurrent at $\lambda = 500$ nm

Conclusions

The electrochemical copolymerization of Py and BT was investigated at a fixed potential of 1.1 V with various monomer ratios. Electrochemical measurements, spectroscopic studies and DSC measurements of the copolymers show that true copolymers were formed.

For the copolymer film a bilayer model is suggested. The value of E_{FB} corresponding to that of the pure PPy at constant potential of −0.64 V was found together with characteristic values of $E_{FB} = -0.34$ V for PyBT10 and $E_{FB} = -0.05$ V for PyBT20. The E_{FB} of the copolymer shifts from that of PPy to PBT with an increase of BT in the copolymer film. The doping concentration N of the copolymer was of the order of 10^{17} cm^{-3}. The results of the impedance measurements were confirmed by photocurrent measurements. Some differences were observed (see Table 3). The band gap

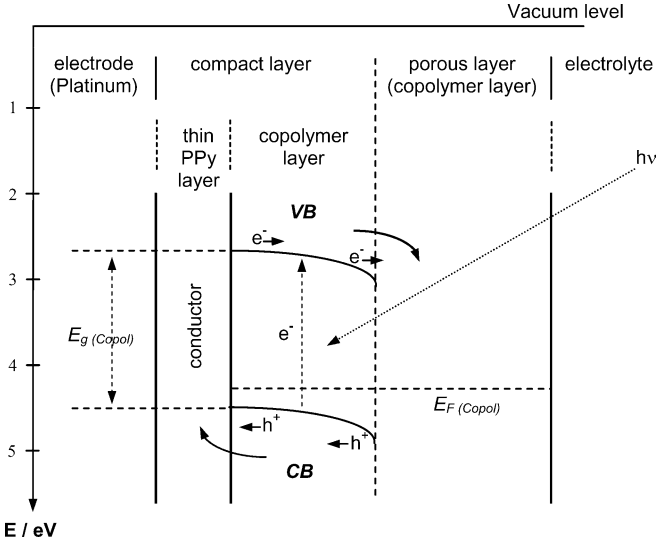

Fig. 10 Energy band diagram of the metal/copolymer as a bilayer/electrolyte (where h^+ is hole, e^- is electron, VB is the valence band and CB is the conductive band). $E_{g\ (Copol)} = 1.97$ eV for PyBT10 and 1.94 eV for PyBT20; $E_{F\ (Copol)} = 4.37$ eV for PyBT10 and 4.63 eV for PyBT20 under $-0.64\ \text{V} < E < E_{FB\ (Copol)}$

energies were derived from photocurrent spectra. Values of $E_g^{di} = 1.97$ eV for copolymer PyBT10 and $E_g = 1.94$ eV for copolymer PyBT20 were found. These values changed with changing copolymer composition. The results of semiconductor characterization were in good agreement with the observed shifts of the redox potentials of the copolymer films as determined by cyclic voltammetry.

Acknowledgements This work was supported by the Deutsche Forschungsgemeinschaft-DFG and the Graduate School Sensorik of the TU Dresden. The authors are greatly indebted to Dr. H. Kroschwitz (Institute of Organic Chemistry, TU Dresden) for ESI MS measurements and for his discussions.

References

1. McCullough RD (1998) Adv Mater 10(2):93
2. Zhang WF, Schmidt Zhang P, Kossmehl G (2001) J Solid State Electrochem 5:74
3. Zhang W, Schmidt Zhang P, Kossmehl G, Plieth W (1999) J Solid State Electr 3:135
4. Chakrabarti S, Banerjee D, Bhattacharyya R (2002) J Phys Chem B 106:3061
5. Fang Q, Chetwynd DG, Covington JA, Toh C-S, Gardner JW (2002) Sensor Actuat B–Chem 84:66
6. Torres W, Fox MA (1992) Chem Mater 4(1):146
7. Peters EM, Van Dyke JD (1991) J Polym Sci A 29:1397
8. Sari B, Talu M (1998) Synthetic Met 94:221
9. Micaroni L, Polo da Fonseca CN, Decker F, De Paoli MA (2000) Sol Energ Mat Sol C 60:27
10. Zhang WF, Schmidt-Zhang P, Kossmehl G (2000) J Solid State Electr 4:225
11. Yang Y, Lin ZG (1994) Synthetic Met 64:43
12. Morgenstern T, König U (1994) Synthetic Met 67:163
13. Aubert PH, Neudeck A, Dunsch L, Audebert P, Capdevielle P, Maumy M (1999) J Electroanal Chem 470:77
14. Ryder KS, Schweiger LF, Glidle A, Cooper JM (2000) J Mater Chem 10:1785
15. Tanaka N (2001) Thermochim Acta 374:1
16. Zarbin AJG, De Paoli MA, Alves OL (1999) Synthetic Met 99:227
17. Liu YC, Hwang BJ (2000) Synthetic Met 113:203
18. Bazzoui EA, Marsault JP, Aeiyach S, Lacaze PC (1994) Synthetic Met 66:217
19. Sauvajol JL, Poussigue G, Benoit C, Lere-Porte JP, Chorro C (1991) Synthetic Met 41–43:1237
20. Funt BL, Peters EM, van Dyke JD (1986) J Polym Sci A 24:1529
21. Rammelt U, Schiller C-A (2000) ACH–Models Chem 137:199
22. Fikus A, Rammelt U, Plieth W (1999) Electrochim Acta 44:2025
23. W. W. Gärtner WW (1959) Phys Rev 116:84
24. Rammelt U, Hebestreit N, Fikus A, Plieth W (2001) Electrochim Acta 46:2363
25. Gerischer H (1990) Electrochim Acta 35(11/12):1677
26. Wilson RH (1977) J Appl Phys 48:4292
27. Girotto EM, Gazotti WA, De Paoli MA (2000) J Phys Chem B 104:6124